Formation of martian araneiforms by gas-driven erosion of granular material

S. de Villiers[1,2], A. Nermoen[1,3], B. Jamtveit[1], J. Mathiesen[1,4], P. Meakin[1,5,6], S.C. Werner[1,7]

1 *Physics of Geological Processes, University of Oslo, Box 1048 Blindern, N0316.*

2 *Now:Sogn og Fjordane University College, Postboks 133, N6851 Sogndal, Norway*

3 *Now:International Research Institute of Stavanger, P.O. Box 8046, N4068 Stavanger, Norway*

4 *Niels Bohr Institute, University of Copenhagen, Copenhagen, Denmark*

5 *Carbon Resource Management Department, Idaho National Laboratory, Idaho Falls, Idaho 83415, USA*

6 *Multiphase Flow Assurance Innovation Center, Institute for Energy Technology, Kjeller, Norway*

7 *Centre for Advance Study at The Academy of Science and Letters, Oslo, Norway*

Correspondence and requests for materials should be addressed to S de Villiers (simondev@hisf.no).

Abstract

Sublimation at the lower surface of a seasonal sheet of translucent CO2 ice at high southern latitudes during the martian spring, and rapid outflow of the CO2 gas generated in this manner through holes in the ice, has been proposed as the origin of dendritic 100m – 1 km scale branched channels known as spiders or araneiforms and dark dust fans deposited on top of the ice. We show that patterns very similar to araneiforms are formed in a Hele-Shaw cell filled with an unconsolidated granular material by slowly deforming the upper wall upward and allowing it to return rapidly to its original position to drive air and entrained particles through a small hole in the upper wall. Straight, braided and quasiperiodic oscillating channels, unlike meandering channels on Earth were also formed.

1. Introduction

Seasonal temperature variations in the polar regions of Mars have created unique landscapes displaying a host of remarkable patterns. Araneiforms consisting of a poorly defined central depression surrounded by a number of branched channels (Fig 1a), are a striking example [*Kieffer et al,* 2006]. They range in size from tens of meters up to about one kilometer, with typical diameters of 200-300m. Channel depths of 0.6 to 1 m have been estimated for typical 5 m wide channels [*Hansen et al*., 2010, *Piqueux et al.,* 2003]. During the martian spring, these unusual patterns are associated with the transient formation of dark fan-shaped dust deposits, which are formed in approximately the same positions each year, indicating that local topographic features are important for their formation [*Thomas et al.,* 2010]. [*Piqueux and Christensen,* 2008] suggested a minimum formation time on the order of 10^4 years, based on estimates of the volume of granular material that must be excavated to form the central depression and the amount of granular material in a typical fan-shaped deposit. A better understanding of araneiform formation is important because it is estimated to be one of the most efficient erosive processes on Mars, displacing two orders of magnitude more dust per year than typical dust storms or than the combined effects of dust devils during the same time period [*Piqueux and Christensen,* 2008].

In addition to the hypothesis that araneiforms are formed by erosive flow of CO_2 produced by solar radiation induced sublimation at the base of an impermeable CO_2 ice cap, [*Hansen et al*., 2010; *Kieffer et al,* 2006], other mechanisms have been proposed including erosion by flowing brine during the martian summer [*Prieto-Ballesteros et al.,* 2006]. However, the varying topography in regions where araneiforms are observed and the lack of associated anisotropy challenges gravity driven flow explanations [*Hansen et al*., 2010]. Since investigations of the formation of araneiforms rely on remote sensing; it is difficult to directly test

hypotheses concerning their formation. Our experiments demonstrate that ramified patterns, similar to araneiforms, are formed by the erosive venting of gas through a hole in the upper plate of a Hele-Shaw cell filled with an unconsolidated granular material (Figs 1b).

2. Experimental system

Experiments were performed in a Hele-Shaw cell consisting of two parallel horizontal glass plates. The upper plate was circular with a diameter of 50 cm and a thickness of 4 mm, and the lower plate was square with a width of 80 cm and a thickness of 2 cm. The plates were separated by a layer of spherical silicate glass beads with a characteristic particle diameter of ≈40 μm (half the mass was in particles with diameters > ≈40 μm). The cell was prepared by uniformly distributing 22 ml of beads to form a roughly circular granular layer with a thickness of 230 μm and a diameter of 35 cm. The cell was open along the outer perimeter between the upper and lower glass plate. Weights, totaling 9 kg were distributed around the perimeter of the upper plate, and a 1 mm diameter hole in the center of the upper plate represented a vent. While the weights held the rim in place, a lifting force, controlled by an electric motor was used to deform the upper plate, via a wire attached to the upper plate near to the 1mm diameter hole, and the force was measured by a scale attached (in series) between the wire and the motor.

An experimental cycle, illustrated in Fig. 2, consisted of: (1) a slow increase in the lifting force, which increased the aperture of the Hele-Shaw cell without changing the structure of the granular layer; and (2) rapid release of the lifting force, which allowed the plate to return to its initial position, closing the aperture, and generating a transient air over-pressure above and within the granular medium. The increase in height at the center of the plate was measured using a linear variable differential transformer, and this enabled us to estimate the rate at which the plate flexed back to its original position during the second stage of the cycle. The Hele-Shaw cell was

illuminated from below, and reduction of the thickness of the granular layer between the glass plates was identified by an increase in brightness in the images that were recorded after each cycle (Fig. 1b).

3. Results

The morphology and dynamical evolution of the pattern were recorded during many lifting and air expulsion cycles, and patterns formed with maximum lifting forces of 20N and 30N are shown in Figs. 1b and 3. For both high and low lifting forces, branching developed by both side-branching and tip-splitting. For low lifting forces, some of the channels were almost straight, while others had a sinuous form, sometimes with very sharp bends (Fig. 3a). When the lifting force was larger, the pattern growth was faster, the channels were wider, the wavelength of the sinuosity was greater, and some braided channels formed (Fig. 3b).

Assuming that the lifting force of $F_{lift} \approx$ 20-30N, is distributed over the area of a well developed experimentally generated araneiform with a radius of ≈ 10cm, we estimate a maximum overpressure of $\Delta P \approx$ 0.6-1 kPa. Since this is much smaller than atmospheric pressure, the gas flow can be considered to be incompressible. For a lifting force of 30 N, the height increased by 55 μm, and the time required for the plate to return to its initial position decreased from $\Delta t \approx$ 1.0±0.1(s.d.) s for early stage pattern formation (low permeability) to $\Delta t \approx 0.6 \pm 0.1$(s.d.) s at later stages (because the channels increased the permeability). Based on estimates of the increase in the cell volume during flexure and measurements of the relaxation time, we estimated that the gas was ejected through the central hole with an average velocity of $v_{release} \approx$ 1 m/s during experiments with a 30 N lifting force.

4. Discussion

Erosion of channels beneath a CO_2 ice sheet on Mars could be driven by sublimation and outflow through preexisting holes in the ice, or by sublimation under an essentially impermeable CO_2 ice sheet which later ruptures producing localized vents. In most studies it has been assumed that the second of these scenarios is dominant. In any event, the observation of dark dust fans deposited on the martian surface indicates a low permeability sheet with a low density of holes. As discussed by [*Kieffer*, 2007, *Portyankina et al.*, 2010], it is not clear whether the entire sheet is lifted or partially lifted by the overpressure, or if the sheet is anchored to the underlying substrate in some locations and is deformed by overpressure beneath the sheet. The experiments were designed to investigate the generation of branched channels in a granular bed by convergent flow driven by a distributed over pressure, towards a hole in an overlying impermeable sheet. On Mars, sublimation under an impermeable CO_2 ice sheet may lift the sheet, and when a vent is formed in the sheet, the sheet falls, driving gas rapidly towards the vent, as in the experiments. However, erosion of the granular bed by convergent flow towards the vent is also expected to generate branched channels whether the sheet is raised or it remains fully or partially attached to the underlying soil

Branched channels, somewhat similar to those associated with araneiforms, and those formed in the experiments are formed when fluid flows through an unconsolidated granular medium towards a hole in a Hele-Shaw cell [*Cerasi et al.*, 1995; *Cerasi and Mills*, 1998]. Branched channels are also formed in soils by outflow erosion (soil sapping and piping) [*Higgins*, 1984; *Jones*, 2004] and via erosion by overland flow [*Schumm*, 1956]. In all of these systems, fluids flow down hydraulic potential gradients towards channels in which the resistance to flow is relatively small. Channel elongation and branching is driven by the convergent flow at the channel tips. The rate of erosion increases rapidly with the quantity of fluid flowing into the channel tips, and the concept of an erosion threshold, below which erosion is slow and above

which erosion is fast, is useful [*Horton*, 1945; *Howard*, 1994]. In the experiment, the aerodynamic forces, f_a, acting on the particles, or clusters of particles, at the interface between the dry unconsolidated granular medium and the open channels must be large enough to overcome the gravitational force, f_g, and/or Van der Waals force, f_{VdW} holding them in place. The aerodynamic force consists of a contribution from gas flowing from the porous medium into the channels and a contribution from the gas flowing over the granular material. Whether the flow in the gap between the CO_2 ice sheet and the martian soil, or the flow in the gap between the glass sheet and in the granular bed in the experiments is laminar or turbulent, the aerodynamic forces acting on the granular bed are largest as the gas flow enters the channel tips.

Channel growth is controlled by the flow of gas into the channel tips, and $Q_{tip} \approx Q/n_{tip,}$ where Q_{tip} is the volumetric flux into a channel tip, Q is the total volumetric flux through the vent and n_{tip} is the effective number of tips. Given this approximation for Q_{tip}, the fluid velocity, the channel width and the channel depth (or the aperture of the gap between the granular bed and the impermeable CO_2 ice or glass sheet), the ratio between aerodynamic and gravitational forces acting on the particles and the ratio between the aerodynamic stress and cohesive strength can be estimated. In the experiments, approximately half of the mass in the granular bed is accounted for by particles with diameters of ≈40 μm or greater. This indicates that the gravitational stress at a depths of 1 particle diameter is greater than or approximately equal to the Van der Waals cohesive strength. Analysis of the experiments indicates that near the channel tips, the aerodynamic drag forces generated by flow over the granular bed are greater than the forces associated with outflow from within the granular pore space, except when the gap between the upper sheet and the granular bed is small, towards the end of a cycle, as the sheet approaches the granular bed. Throughout most of the second half of the cycle, when the top sheet is falling, $f_a \approx$

$0.01 f_g$ and $f_g \geq f_{VdW}$, where f_a is the aerodynamic force near the channel tips estimated assuming that $n_{tip} \approx 50$. It is surprising that channels are formed when f_a / f_g is so small, and this may be related to the ease with which nearly spherical particles can be moved over the smooth glass bottom wall of the Hele-Shaw cell. In principle, this provides a way of quantitatively comparing the experiments and martian araneiforms through dimensionless ratios such as $\Pi_1 = Q\eta/(\rho_s g d^2 h w_{tip})$ for outflow erosion, $\Pi_2 = Q\eta/(h_g^2 w_{tip} \rho_s g d,)$ for erosion due to laminar flow over the granular bed and $\Pi_3 = [\rho_f \{Q/(h_g w_{tip})\}^2/(\rho_s g d)] f(Re)$ for turbulent flow over the bed, where η is the fluid viscosity, h_g is the gap height, w_{tip} is the channel width near the tip, ρ_s is the particle density, ρ_f is the fluid density, g is the gravitational acceleration, d is the particle diameter, and $f(Re)$ is a function of the Reynolds number, Re. In principle, a computational or physical model will reproduce the behavior observed in nature if $\{\Pi^{mod}\} \equiv \{\Pi^{obs}\}$, where $\{\Pi^{mod}\}$ and $\{\Pi^{obs}\}$ are complete sets of dimensionless ratios in the observed and model systems. In practice, it is sufficient if some of the dimensionless ratios are large or small enough. For example, if $d/h_g << 1$, $d/w_{tip} << 1$, $d/L << 1$, $d/h_b << 1$ in both the model and observed system and the other dimensionless ratios are sufficiently similar, where L is the scale of the branched channel network and h_b is the depth of the granular bed, the model and observed systems will exhibit essentially the same behavior. In practice, $d/w_{tip} << 1$ and $d/L << 1$, but $d/h_b \approx 0.17$, and $d/h_g \approx 1$. However, the dimensionless ratios that characterize the relative magnitudes of aerodynamic and gravitational or cohesive forces are much more important, and even the relatively large values of d/h_b and d/h_g may be sufficiently small. Unfortunately, there are significant uncertainties in the experiments (we estimated, but could not measure, the velocity of the upper plate and the permeability of the granular bed) and much larger uncertainties on Mars. In particular, while there is some information about the particle size distribution and the cohesive strength of martian

sediments at the Rover and Viking lander sites, there are large uncertainties in the effective depth and permeability of the martian soil in the regions in which araneiforms have been observed. In addition the nature of the gap between the CO_2 ice and the martian soil, the physical properties of the CO_2 ice sheet, and the cementing of soil particles by CO_2 and/or H_2O ice within the sediments are also highly uncertain.

In the experiments, the depth averaged transport of gas through the gap and the granular bed can be described in terms of a pressure diffusion equation with a source term representing the motion of the upper wall of the Hele-Shaw cell. On Mars, gas is expected to flow through the martian soil and through the gap between the CO_2 ice and the soil (if any), but sublimation provides the source term. Because the gas flow can be described by a pressure diffusion equation, the formation of araneiforms is related to diffusion limited aggregation and other Laplacian growth processes, and araneiforms superficially resemble the convergent branched patterns generated by Laplacian growth [*Meakin, 1998*]. However, araneiforms are commonly connected (Fig 1a), which is not expected for a simple pressure diffusion controlled process, and this may be related to changes in the vent positions over time, and temporal differences in the activation of adjacent vents.

The average separation between adjacent channels, l_c, (the inverse of the drainage density in a fluvial system) is an important characteristic length in experimental branched patterns. In an idealized experimental system or model, this characteristic length is given by $l_c = (b^3\sigma_y/(12\dot{b}\mu))^{1/2}$, where b the gap between the plates, σ_y, is the cohesive strength of the sediments, $\dot{b}$, is the rate at which the gap between the plates is reduced (or the rate at which gas is produced) and μ is the gas viscosity (Supplement 1). A detailed study of characteristic length

scales observable on martian araneiforms would require extensive 3D analysis of araneiforms, which is beyond the scope of this study.

It is tempting to compare changes in the araneiform like patterns produced during an experiment as the number of iterations increases (Fig. 3) with differences between araneiforms of different sizes observable on Mars, a few examples of which are visible in Figure 1a. Additional experiments are required in order to ascertain if there is a morphological difference between patterns whose sizes are limited by the number of erosive iterations as opposed to those whose sizes are limited by the experimental system size or other external factors such as encroachment of channel systems from neighbouring vents.

During an experiment, erosion rates are largest at the channel tips. Within the channels, where the gas flow velocity is relatively small and the gas flux density from the granular bed into the channels is small, the erosion rate is very small, and channel elongation occurs with little or no channel broadening. However, as channels converge near to the vent, the gas velocity increases, and this results in channel broadening as the vent is approached (Figs. 1 and 3). This, as well as changes in the vent position from year to year, may contribute to the large eroded regions near the centers of martian araneiforms (Fig 1a).

In the experiments, sinuous channels (Fig. 3a) form when low or moderate forcing, corresponding to a moderate gas discharge rate, is applied to the upper glass plate (Fig. 3a). The channels are less sinuous than meandering streams in alluvial fluvial systems on Earth, and cutoffs are not formed. This combined with the low density of the fluid and small channel size may be a consequence of confinement of the flow by the overlying ice sheet, which would inhibit the secondary circulation, perpendicular to the flow velocity averaged across the channel [*Leliavsky*, 1955], which is a characteristic of open channel flow on Earth. Undulating channels

are abundant in the araneiform patterns on Mars (Fig. 2a) implying that there are phases during their formation in which granular material is both deposited and eroded.

If large pulling forces are applied to the upper plate (Fig. 3b), the undulations are suppressed, and channels similar to braided river systems develop (Fig. 3b). This behavior resembles that observed in fluvial systems on Earth where channels with larger bed slopes and higher sediment loads have braided forms, and channels in which the flow is less strongly driven by gravity and the sediment load is smaller have meandering forms [*Schumm,* 1985].

5. Conclusions

1. The experiments demonstrate that the erosion of granular material caused by pressure gradient driven gas flow and venting produces convergent dendritic patterns that are similar to martian araneiforms and thus supports the hypothesis that these features are produced by the venting of CO_2 gas during the martian spring.

2. Quasiperiodic sinuous channels, which are not like meandering channels on Earth, and braided channels were observed in the experiments. Similar features are seen in martian araneiforms, but they are not as distinct, possibly because of heterogeneity in the martian soil, and year to year wandering in the position of the vent.

Acknowledgements

The authors gratefully acknowledge the comments and suggestions of Ganna Portyankina and an anonymous reviewer. The experimental work was supported by O. Gunderson and R. G. de Villiers. This study was funded by a Center of Excellence grant from the Norwegian Research Council to Physics of Geological Processes.

References

Cerasi, P, P. Mills, (1998), Insights in erosion instabilities in nonconsolidated porous media,

Physical Review, **E85**: 6051-6060, DOI: 10.1103/PhysRevE.58.6051.

Cerasi, P, P. Mills, S. Fautrat (1995), Erosion instability in a nonconsolidated porous medium, *Europhysics Letters*, **29**: 215-220, DOI: 10.1209/0295-5075/29/3/005.

Jones, J. A. A. (2004), Pipe and Piping in Goudie, A. S., Editor, *Encyclopedia of Geomophology*, Volume 2, Routledge (Taylor and Francis) London, pages 784-788

Hansen, C. J., *et al*. (2010), HiRISE observations of gas sublimation-driven activity in Mars' southern polar regions: I. Erosion of the surface. *Icarus* **205**, 283-295, DOI: 10.1016/j.icarus.2009.07.021.

Higgins, C. G. (1984), *Piping and sapping: development of landforms by groundwater outflow in LaFleur*, R. G., Editor, Allen and Goodwin, New York, pages 18-58.

Horton, R. E. (1945) Erosional development of streams and their drainage basins – hydrophysical approach to quantitative morphology, *Geological Society of America Bulletin*, 56, 275-370, DOI 10.1130/0016-7606(1945)56[275EDOSAT]2.0.CO.2

Howard, A. D. (1994), A detachment-limited model of drainage basin evolution., Water Resources Research, **30**, 2261-2285, DOI: 10.1029/94WR00757.

Kieffer, H. H., P. R. Christensen, T. N. Titus (2006), CO_2 jets formed by sublimation beneath translucent slab ice in Mars' seasonal south polar ice cap. *Nature* **442**, 793-796, DOI: 10.1038/nature04945.

Kieffer, H. H., (2007), Cold jets in the Martian polar caps. *J. Geophys. Res.* **112** E08005, DOI: 10.1029/2006JE002816.

Leliavsky, S., (1955) *An introduction to fluvial hydraulics*, Constable & Company, London.

Meakin, P., (1998), *Fractals, scaling and growth far from equilibrium*, Cambridge University Press, Cambridge, UK.

Piqueux, S., S. Byrne, M. I. Richardson (2003), Sublimation of Mars's southern seasonal CO_2 cap and the formation of spiders. *J. Geophys. Res.* **108**, 5084, DOI: 10.1029/2002JE002007.

Piqueux, S. and Christensen P. R. (2008) North and south subice gas flow and venting of the seasonal caps of Mars: A major geomorphological agent, *J. Geophys. Res*, **113**, E06005, DOI: 10.1029/2007JE003009.

Portyankina, G., Markiewicz, W. J., Thomas, N., Hansen, C. J., Milazzo, M. (2010) HiRISE observations of gas sublimation-driven activity in Mars' southern polar regions: III. Models of processes involving translucent ice, *Icarus* **205**, 311-320, DOI: 10.1016/j.icarus.2009.08.029.

Prieto-Ballesteros, G., C. Fernandez-Remolar, J. A. Rodriguez-Manfredi, F. Selsis, S. C. Manrubia, (2006), Hypothesis paper - Spiders: Water-Driven Structures in the southern hemisphere of Mars, *Astrobiology* **6**(4), 651-667, DOI: 10.1089/ast.2006.6.651.

Schumm, S. A. (1956), Evolution of drainage systems and slopes in badlands at Perth Amboy, New Jersey, Geological Society of America Bulletin 67, 597-646 DOI: 10.1130/0016-7606(1956)67 [597:EODSAS]2.0.CO.2

Schumm, S. A., (1985), Patterns of alluvial rivers. *Annu. Rev. Earth Planet. Sci*. **13**, 5-27, DOI: 10.1146/annurev.ea.13.050185.000253.

Smith, D. E., M. T. Zuber, and G. A. Neumann (2001), Seasonal variations of snow depth on Mars, Science, 294, 2141 – 2146, DOI:10.1126/science.1066556.

Thomas, N., C. J. Hansen, G. Portyankina, P. S. Russell (2010), HiRISE observations of gas sublimation-driven activity in Mars' southern polar regions: II. Surficial deposits and their origins. *Icarus* **205**, 296-310, DOI: 10.1016/j.icarus.2009.05.030.

Figure 1 | Martian araneiforms and experimentally-produced branching patterns.

a) Martian araneiforms after the seasonal CO_2 has sublimed. **b)** A pattern produced in the laboratory by cyclic venting.

Figure 2 | Experimental Setup. Schematic representation of stage 1 of the experimental cycle, in which the lifting force applied to the upper plate is slowly increased, and stage 2 of the experimental cycle, in which the force applied to the upper plate is rapidly reduced.

Figure 3 | Evolution of ramified erosion patterns in an unconsolidated granular medium confined in a Hele-Shaw cell. Rows 1-3: Two experiments at different stages of pattern formation with pulling forces of (a) 20 N and (b) 30 N. The stage of formation is defined by the number of times the upper plate was raised and released. For larger pulling forces a larger volume of gas was expelled during each cycle, and the fingers were broader and straighter. Row 4, left hand side: Details of Fig. 2a, displaying tip-splitting, side-branching and the development of undulations as the araneiform arms grow using the lower pulling force. Row 4, right hand side: Details of Fig 2b displaying side branches and grains deposited within a channel, after the 150^{th} venting event during an experiment using the higher pulling force.

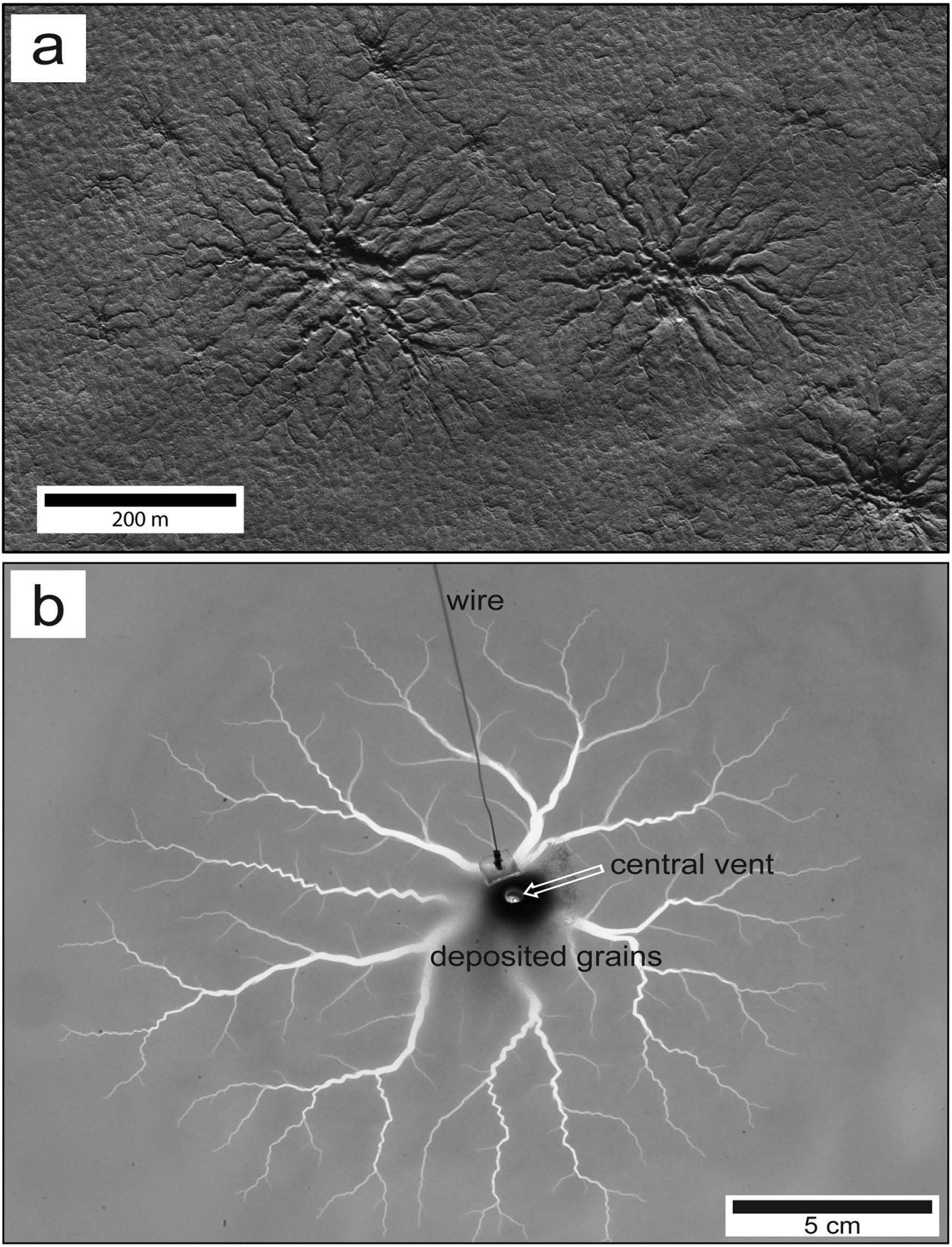
a
200 m
b
wire
central vent
deposited grains
5 cm

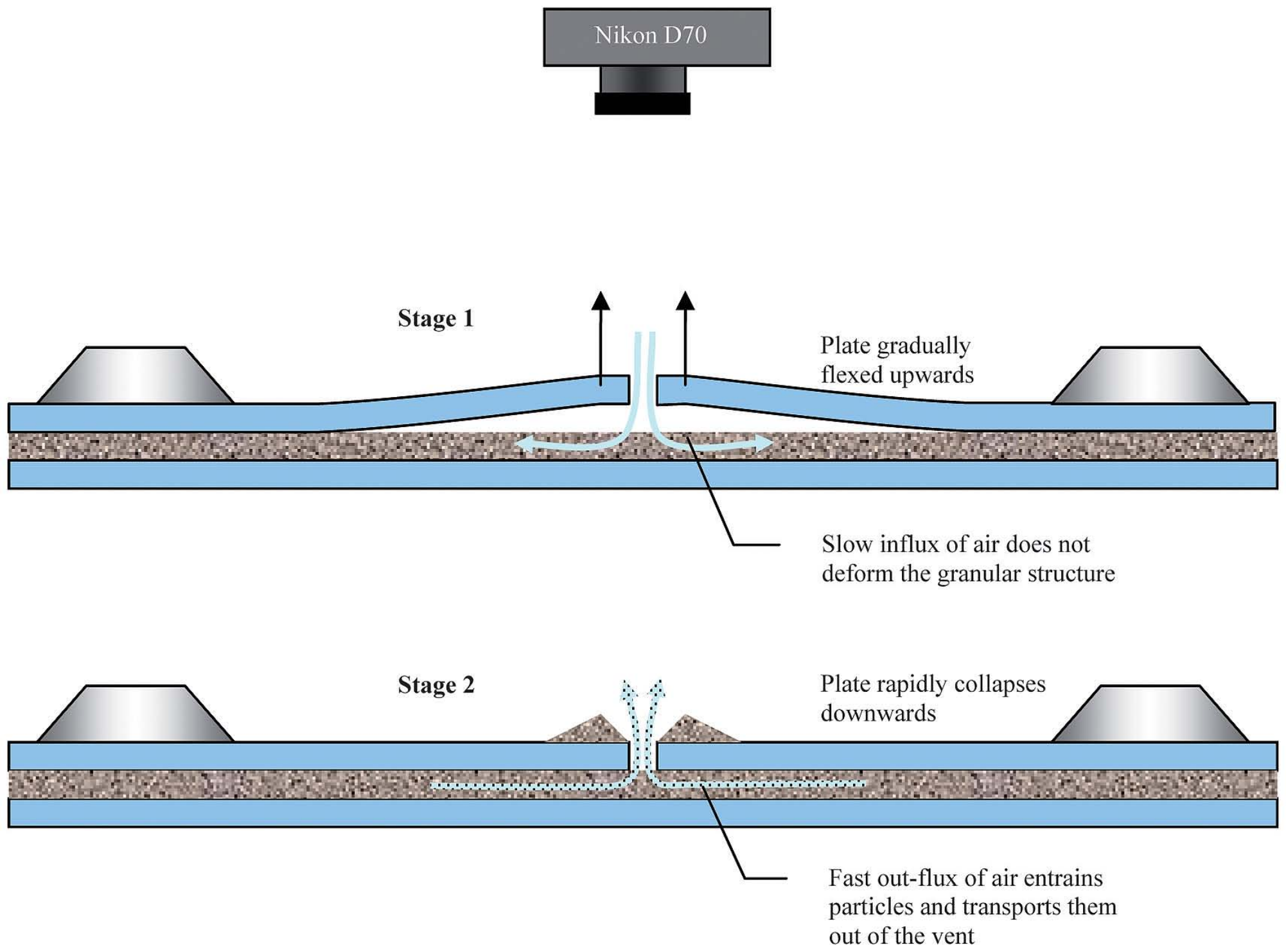
Nikon D70
Stage 1
Plate gradually
flexed upwards
Slow influx of air does not
deform the granular structure
Stage 2
Plate rapidly collapses
downwards
Fast out-flux of air entrains
particles and transports them
out of the vent

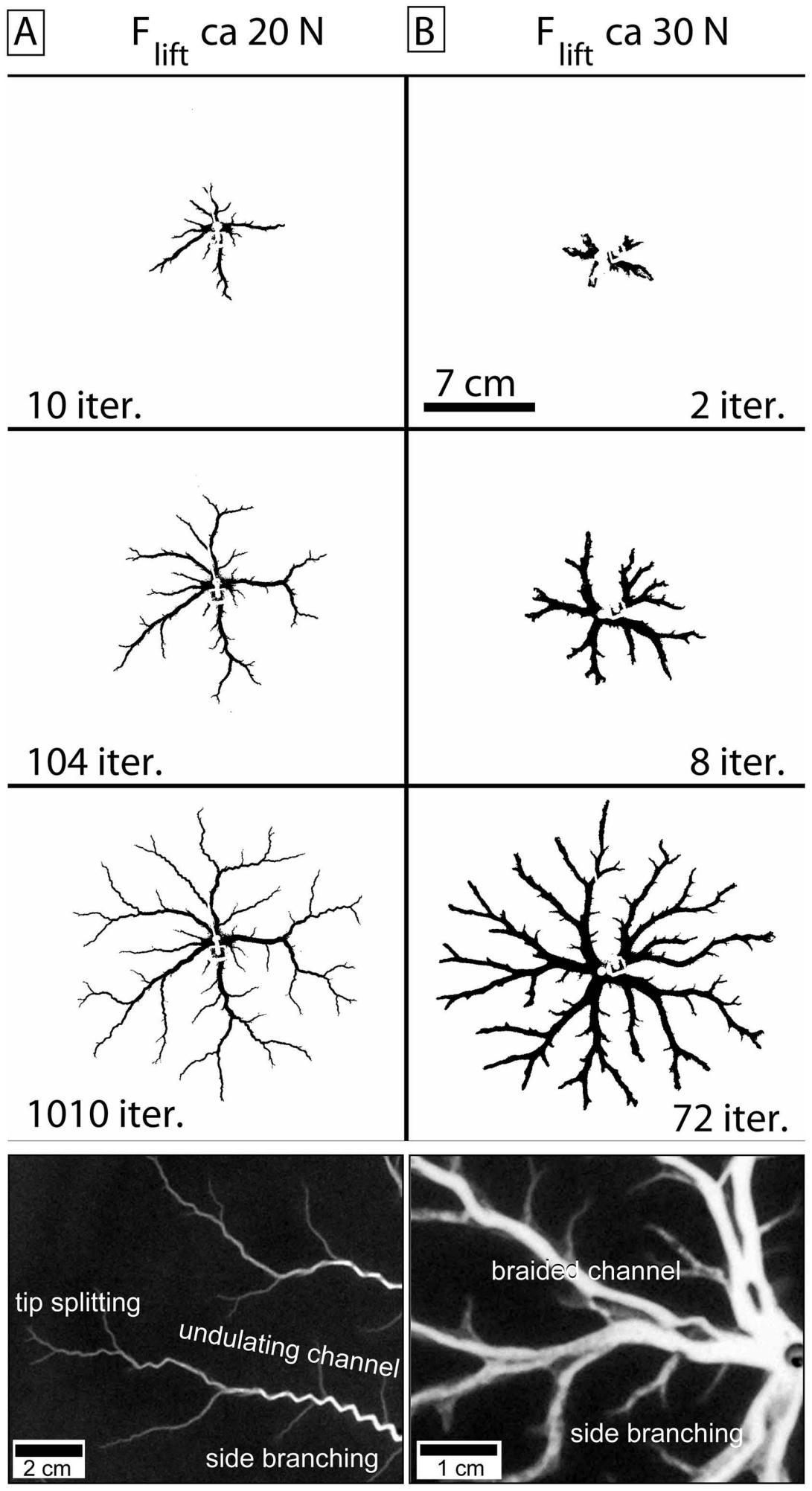
A
F lift ca 20 N
B
F lift ca 30 N
10 iter.
7 cm
2 iter.
104 iter.
8 iter.
1010 iter.
72 iter.
tip splitting
undulating channel
side branching
2 cm
braided channel
side branching
1 cm